End Effector Control System of 6R Manipulator Based on Fuzzy PID

Junpeng Xu

School of electrical engineering and information, Southwest Petroleum University, Chengdu, China.

201931072433@stu.swpu.edu.cn

Abstract. The front three axes of a traditional 6R manipulator move and the back three axes rotate. Given that it is directly connected with the end effector to work and there are some factors such as motor weight, inertia, and material, the end of the manipulator is designed as a system with springs and dampers, so as to improve the stability of the manipulator, reduce errors, and improve production efficiency. Conventional PID control often determines the proportional, integral, and differential effects through simulation, which can not well control the 6R manipulator system in a nonlinear and time-variant state. In order to control the system better, in addition to designing a fuzzy PID control system by making relevant membership functions and fuzzy rules, this paper simulates the end effector of the 6R manipulator by Simulink. The simulation results show that compared with conventional PID, fuzzy PID has better indexes in rapidity, stability, accuracy, and adaptability. The end effector control system of the 6R manipulator based on fuzzy PID is more stable and accurate than the ordinary 6R manipulator.

Keywords: 6R Manipulator; End Effector; Fuzzy PID; Adaptability.

1. Introduction

6R manipulator has come out for a long time, which has greatly promoted the development of human beings as the core equipment of spacecraft on-orbit assembly and maintenance. Thanks to its integrated space sensing, maneuvering, and operation capabilities, it can complete on-orbit assembly, pollution cleaning, observation and inspection, fault module replacement, and on-orbit filling of spacecraft through on-orbit operation, ground remote control, or autonomous operation. Moreover, work including consumption load replacement and replenishment, orbit clearing, orbit transfer, etc. also can be finished by the 6R manipulator[1]. The experience of building and maintaining the International Space Station tells us that using space manipulator to assist astronauts to complete tasks such as space building and load maintenance greatly reduces the risk of astronauts leaving the cabin, reduces the working pressure of astronauts, and automatically deals with some emergencies, which improves the efficiency of space exploration activities [2-5]. Installing solar panels requires high precision and stability of manipulators in aerospace. In some working processes, the inertia of the traditional 6R manipulator is large due to the overweight steering gear and material strength, which leads to side effects such as vibration and overshoot, resulting in unnecessary wear, the increasing costs of space exploration, and even potential accidents.

To improve the precision and safety of the traditional manipulator, it is crucial to modify the end of the 6R manipulator. This paper takes the most classical PUMA-560 as an example to study the modification of the end effector. The first three joints of PUMA-560 from American Unimation Company are mainly used to realize three displacement degrees of freedom, while the last three joints' rotational freedom of the same Z axis easily solves the inverse motion known as Pieper's solution. As the place where it contacts the outside world most, the end of the manipulator is designed as a system with double spring dampers and then connected with various end effectors to perform diverse tasks. Only the last coordinate system in the D-H table is changed. Specifically, when connecting each end effector, the length of the system is extended in the Z axis and the other relative relations remain unchanged, thus achieving better portability. Meanwhile, considering the complex working conditions of the 6R manipulator in aerospace operation, the traditional PID control strategy is

difficult to achieve good control accuracy requirements. Thus, a control method based on fuzzy PID is adopted. By observing the stability, anti-interference, and accuracy of the external force on the end of the manipulator and the displacement it causes, it is proved that the double-spring mass system can buffer the force on the end of the manipulator to enhance the stability and reduce the error.

Firstly, this paper analyzes the double-spring mass system and proves the feasibility of reforming the end of the 6R manipulator in principle before deducing the mathematical model of the system. By analyzing the transfer function, that is, the relationship between the external force and the displacement of the manipulators' end effector, it testifies that the end effector control system of the 6R manipulator based on fuzzy PID can buffer and isolate to improve the stability. Then, the advantages and disadvantages of fuzzy PID control strategy and conventional PID control strategy are analyzed by simulation, which is concluded that the manipulator controlled by fuzzy PID has better accuracy, stability, rapidity, and adaptability. Finally, the development of 6R manipulator technology has been prospected.

2. Double-spring Mass System

2.1 Feasibility Analysis

Since the design is only carried out at the end of the manipulator, the relative positions of the six joints of the manipulator, that is, the Transformation Matrix between each coordinate system remain unchanged. The only change is the coordinates of the end effector in the last coordinate system because the length of the double-spring mass system is increased in the Z-axis direction.

In this paper, some reasonable hypotheses for manipulator modeling are as follows. 1) All parts of the 6R manipulator are regarded as rigid bodies;2) All joints of the 6R manipulator are in the corresponding center; 3) The friction in the movement is ignored;4) Figure 1.1.1 and Figure 1.1.2 show the initial position and postures of the manipulator.

The parameters of designing the manipulator are as follows. The 6R manipulator and the improved the 6R manipulator are built by the improved D-H method (Craig Vision). It can be seen that only in the last coordinate system {6}, the coordinates of the end effector will stretch the length of the system on the Z axis due to the double-spring mass system, while the other relative relations remain unchanged. Therefore, it not only increases the force on the end of the manipulator but also takes into account the cost without a new manipulation strategy. Its trajectory planning and dynamic analysis are consistent with the previous ideas.

The establishment of the D-H coordinate system and DH Table are shown in Figures 1.1.1-1.1.2 and Table 1.1.1.

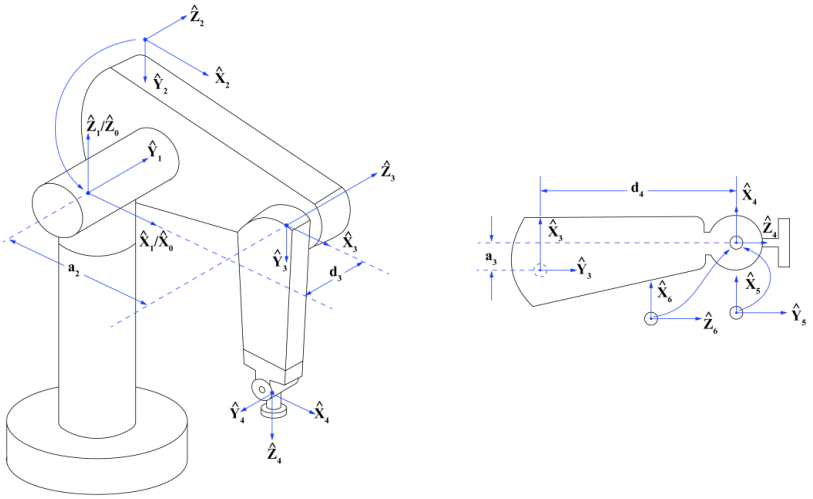

Fig. 1.1.1 Coordinate System Diagram of 6R Manipulator

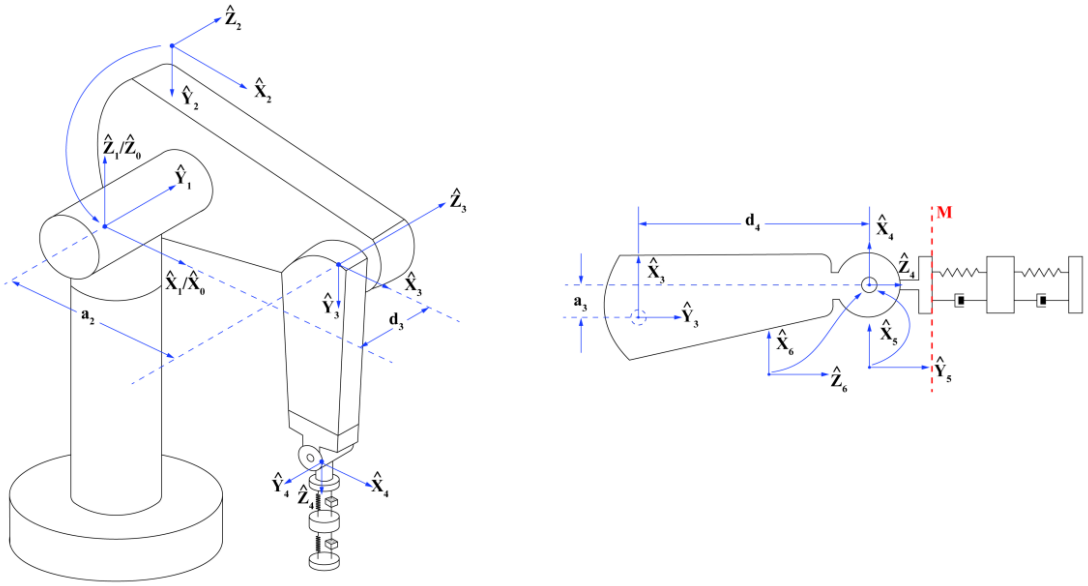

Fig. 1.1.2 Coordinate System Diagram of Improved 6R Manipulator

Table 1.1.1. 6R Manipulator D-H Table/Improved 6R Manipulator D-H Table

i	α_i	a_i	d_i	θ_i
1	0 °	0	0	θ_1
2	-90 °	0	0	θ_2
3	0 °	a_2	d_3	θ_3
4	-90 °	0	d_4	θ_4
5	90 °	0	0	θ_5
6	-90 °	0	0	θ_6

According to the DH Table, Figures 1.1.1 and 1.1.2, under the unchanged posture of the end effector of the manipulator, the origin of its installation position only changes in the direction of the Z6 axis, that is, a spring mass system is added behind the M plane in the figure, which extends the length of the system. Then each Transformation Matrix can be deduced to pull back the geodetic coordinate system. Finally, trajectory planning can be carried out, which proves the feasibility of the system.

The improved 6R manipulator counteracts the force received by the end of the manipulator when working by springs and dampers to achieve buffering and improve stability. The principle of its control system is shown in Figure 1.1.3.

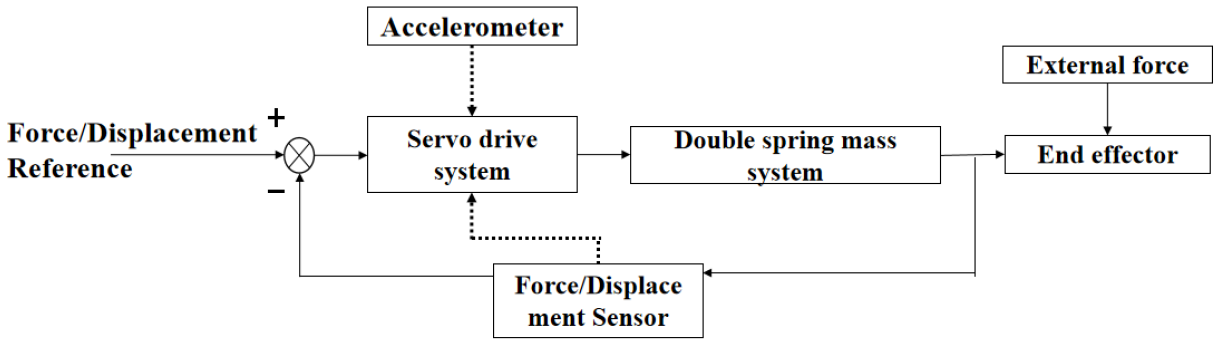

Fig.1.1.3 Schematic Diagram of Control System

2.2 System Architecture

Table 1.2.1. Energy Storage Elements Table

Energy Storage Element	Capacitance C	Inductance L	Mass M	Moment of Inertia J	Spring k
Energy Equation	$1/2\ Cu\hat{}2$	$1/2\ Li\hat{}2$	$1/2\ Mv\hat{}2$	$1/2\ Jw\hat{}2$	$1/2\ kx\hat{}2$
Physical Variable	Voltage u	Current i	Speed v	Angular Velocity w	Length Change x

Common energy storage elements and corresponding energy equations are shown in Table

In 2002, Liu of Tamkang University in Taiwan put forward a compliant tool rack for mold polishing, which uses linear springs to enhance the compliance of equipment, that is, to change the contact flexibility before reducing the surface roughness of the mold [6]. With this as a reference, this design adopts a buffer system composed of springs and dampers, in which springs and mass blocks are energy storage elements, springs store kinetic energy, and mass blocks store potential energy. Because the damper itself is a device that produces viscous friction or damping, it is composed of a piston and cylinder filled with oil, which is mainly used to absorb the energy of the system. The absorbed energy will eventually be converted into heat and dissipated. The damper itself does not store any kinetic energy and potential energy, so the system has four energy storage elements (two springs and two mass blocks).

The improved 6R manipulator is shown in Figure 1.1.2.

2.3 Establishment of Mathematical Model

According to the properties of the Transformation Matrix and Newton's Law, the M plane in Figure 1.1. 2 can be used as a reference to simplify the mechanical analysis of the double-spring mass system and push it back to the geodetic coordinate system through the Transformation Matrix. Assuming that the end of the manipulator works in the same horizontal plane, that is, gravity is not considered, the following derivation is carried out. Due to the similar derivation process of gravity, this paper only demonstrates the system without gravity.

The manipulator can perform different tasks with different end effectors. This paper takes the pneumatic mechanical claw installed on the manipulator as an example to analyze.

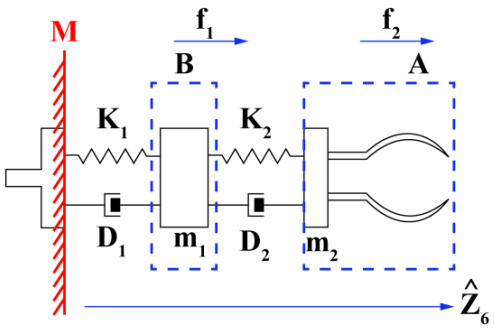

Fig. 1.3.1 Double-Spring Mass System Diagram

The double-spring mass system is shown in Figure 1.3.1. The displacement of the end part B of the manipulator (connected with the spring damper) under the acting force f_1 is x_1, and its mass is m_1; Part A (including the end effector) produces displacement f_2under the acting force x_2, and its mass is m_2. The elastic coefficients of springs are K_1, K_2, while the damping coefficients of dampers are D_1, D_2. All the above are in the right direction and the springs are in an elongated state.

In this paper, only the ideal case is analyzed. It is stipulated that the damping produced by the damper is proportional to the velocity of the object, with the ratio as the damping coefficient. It is

assumed that the velocity of part A is greater than that of part B (x_2>x_1), and other cases can learn from it without further analysis.

The mathematical model is established as follows.

Based on Newton's second law fm=a, the differential equation is established as follows.

For the end B part of the manipulator:

$$m\_1\ (d\hat{}2\ x\_1)/(dt\hat{}2\ ) = f\_1 + K\_2\ (x\_2 - x\_1\ ) + D\_2\ ((dx\_2)/dt - (dx\_1)/dt) - K\_1\ x\_1 - D\_1\ (dx\_1)/dt \quad (1\text{-}1)$$

For the end A part of the manipulator:

$$m\_2\ (d\hat{}2\ x\_2)/(dt\hat{}2\ ) = f\_2 - K\_2\ (x\_2 - x\_1\ ) - D\_2\ ((dx\_2)/dt - (dx\_1)/dt) \quad (1\text{-}2)$$

Only under the condition of zero initial, the Laplace transform is performed on $1-1$ and $1-2$ as follows.

$$m\_1\ s\hat{}2\ X\_1\ (s) = F\_1\ (s) + K\_2\ [X\_2\ (s) - X\_1\ (s)] + D\_2\ s[X\_2\ (s) - X\_1\ (s)] - K\_1\ X\_1\ (s) - D\_1 \quad (1\text{-}3)$$

$$m\_2\ s\hat{}2\ X\_2\ (s) = F\_2\ (s) - K\_2\ [X\_2\ (s) - X\_1\ (s)] - D\_2\ s[X\_2\ (s) - X\_1\ (s)] \quad (1\text{-}4)$$

Without losing generality, assuming $F\_1\ (s) = 0$ based on $1-3$

$$X\_1(s) = \frac{(D_2 s + K_2)X_2(s)}{M_1 s^2 + (D_2 + D_1)s + K_1 + K_2} \quad (1\text{-}5)$$

Substitute 1-5 into 1-4 to get

$$(m_1 s^2 + (D_2 + D_1)s + K_1 + K_2)(m_2 s^2 + D_2 s + K_2)X_2(s) = (m_1 s^2 + (D_2 + D_1)s + K_1 + K_2)F_2(s) + (K_2 + D_2 s)^2 X_2(s) \quad (1\text{-}6)$$

Then there is the system transfer function:

$$(s) = \frac{X_2(s)}{F_2(s)} = \frac{m_1 s^2 + (D_2 + D_1)s + K_1 + K_2}{(m_1 s^2 + (D_2 + D_1)s + k_1 + k_2)(m_2 s^2 + D_2 s + K_2) - (K_2 + D_2 s)^2} \quad (1\text{-}7)$$

Without losing generality, X_1can be obtained by eliminating X_2in (1)and substituting it in (2) to deduce the overall displacement X_1+X_2 of the end effector of the manipulator, which can be pushed back to the geodetic coordinate system. Only the end A of the manipulator is considered without other deductions. According to the transfer function, the stability, anti-interference, and accuracy of the manipulator can be observed by the external force f2 and the displacement X_2 caused by it.

If $m_1 = m_2 = 1\text{kg}$, $D_1 = D_2 = 1\text{N} \cdot \text{s/cm}$, $K_1 = K_2 = 1\text{N/cm}$, we can obtain

$$(s) = \frac{s^2 + 2s + 2}{s^4 + 3s^3 + 4s^2 + 2s + 1} \quad (1\text{-}8)$$

3. Conventional PID Control

3.1 PID Control Principle

PID control algorithm is a control algorithm combining proportions, integrals, and differentials. As the most mature and widely used control algorithm in continuous and discrete systems, it constitutes a control algorithm according to the relationship between the given value and the actual output value. Appearing in the 1930s to 1940s, it is suitable for the situation where the model of the controlled object is unclear. Practical operation experience and theoretical analysis show that this control law can be used to control many industrial processes with satisfactory results.

The traditional 6R manipulator position PID control system is shown in Figure 2.1.1.

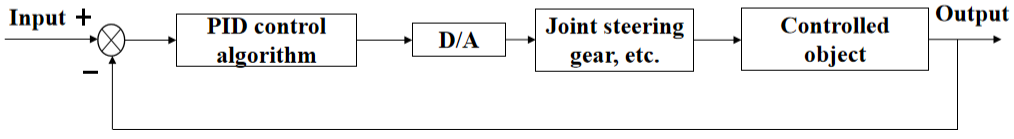

Fig. 2.1.1 Position PID Control System Diagram of Traditional 6R Manipulator

The PID control algorithm is shown in Figure 2.1.2.

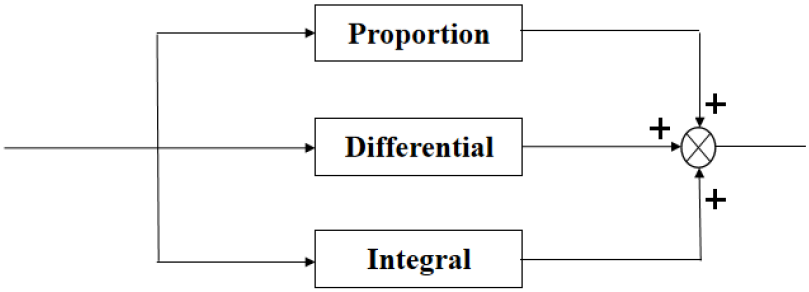

Figure. 2.1.2 PID Control Algorithm Diagram

Thus, the PID control formula is shown as follows.

$$u(t) = K_p\left[e(t) + \frac{1}{T_i}\int_0^t e(t)dt + T_d\frac{de(t)}{dt}\right] \quad (2\text{-}1)$$

Where $u(t)$ is the control quantity output by the controller; $e(t)$ as a deviation signal is equal to the difference between a given quantity and the output value; K_p is the proportional coefficient; $T_i$is the integral time constant; T_d is a differential time parameter.

3.2 Proportional Action

Proportional action can be regarded as a spring between the target point and the controlled object. The farther away the current position is from the target position, more force is needed to make the controlled object return to the target position, which tends to pull the controlled object to the balance position. Once the deviation occurs, the proportion immediately produces a control effect to reduce the error. However, because the controlled object itself has certain inertia, although there is no force when reaching the target point, it will deviate from a certain distance, that is, overshoot will occur. The larger P, the harder the spring, the faster the recovery speed, and the higher the oscillation frequency. However, if there is only proportional action in the closed-loop control, the final result is that the controlled object is repeatedly in a state of over-correction and continues to oscillate endlessly like a pendulum.

To sum up, proportional action can speed up the adjustment of the system, which is essential for coarse adjustment and rapid adjustment. As the main part of shortening the distance from the target value, it focuses on narrowing the current gap but still with steady errors.

3.3 Integral Action

Integral action refers to integrating the deviation between the output and the input of the controller. Integral action can eliminate the error, and it only works under the condition of stable external interference/system error. The greater the deviation, the greater the duration and the correction force. Proportional action is controlled by deviation. Only when there is deviation can there be control; The integral function is to use the accumulation of deviations to produce control. As long as deviations exist, there will always be control. Taking the team following the car as an example, the proportional control depends on whether the speed is consistent, while the integral action depends on whether the distance between cars changes. When the distance between cars is not 0 and the speed difference is 0, the integral action is still controlled to reduce the distance between cars.

To sum up, integration can count errors and understand the past. Although it can eliminate static error, it can also reduce the response speed of the system and increase the overshoot of the system.

3.4 Differential Action

Differential action refers to the differential operation of input deviation, which can be regarded as a buffer solution. The greater the differential action, the greater the resistance of object movement, which is opposite to the direction of object movement; When the differential action is too large, the resistance will cancel out the restoring force. Increasing differential action can effectively reduce

overshoot, but increasing resistance will also make it dull. Differential action is helpful to reduce overshoot, overcome oscillation, speed up tracking, and improve stability. But the differential is very sensitive to the noise of the input signal. For the noisy system, the differential is usually not used or the signal is filtered before the differential takes effect.

To sum up, differential action can improve performance, increase inertial response speed, and weaken the overshoot trend.

4. Fuzzy PID Control

4.1 Fuzzy PID Automatic Control Strategy

Conventional PID control has been able to solve many problems and is widely used in linear time-invariant systems. However, in some control processes, the controlled system is not linear and time-invariant. For example, in the working process of the 6R manipulator in this paper, the traditional PID control is often based on experience, and once the action intensity is determined, it will not change. Therefore, its control function is weakened for the dynamic system, and it fails to meet the requirements in rapidity, accuracy, stability, and adaptability. Therefore, the end effector control system of the 6R manipulator based on fuzzy PID is studied to adapt to the complex and frequent changes in environmental conditions.

Considering that the counterweight device of the 6R manipulator is heavy and easy to overshoot when it works, and the working environment is complex, the detection of sensors is not necessarily accurate. If conventional PID control is adopted, it is difficult to eliminate the complex working conditions in the control system, so fuzzy PID control with better self-adaptability is adopted. Fuzzy PID control in the practical application can reduce the displacement sensor measurement error caused by the end effector instability and better match the spring-mass system to achieve the role of buffering and damping. The control principle is shown in Figure 3.1.1. The inputs in the fuzzy adaptive PID controller e, e_crespectively represent the force deviation and its change rate when the end effector of the manipulator acts with the outside world. By taking $\Delta k_p, \Delta k_i, \Delta k_d$as the fuzzy output variables by fuzzification and fuzzy reasoning, the PID parameters are corrected by real-time detection of force action and deviation value in the process of control, so as to realize the buffer control of the end effector of the 6R manipulator.

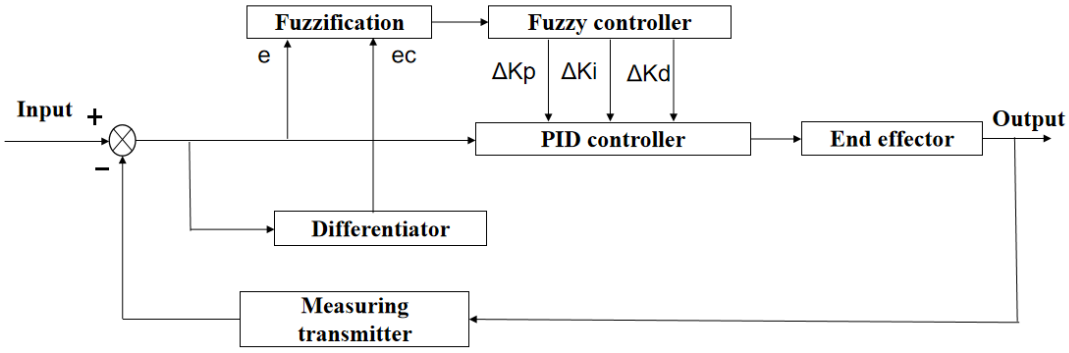

Fig. 3.1.1 Fuzzy PID Control Schematic Diagram

4.2 Fuzzy Rules and Functions

Fuzzy PID control includes three parts including fuzzification, determination of fuzzy rules (fuzzy reasoning), and resolution of fuzziness (clarifications). Fuzzy PID control is widely used in nonlinear systems. For example, the 6R painting manipulator collects and sets the painting line through sensors. In addition to determining the deviation distance (e) between the paint gun and its setting line as well as the change (e_c) of the current and the last deviation, it also makes fuzzy reasoning according to the given fuzzy rules. Finally, it resolves the fuzzy parameters, outputs PID control parameters, and then controls the whole painting process.

The basic principle of fuzzy PID control is shown in Figure 3.2.1

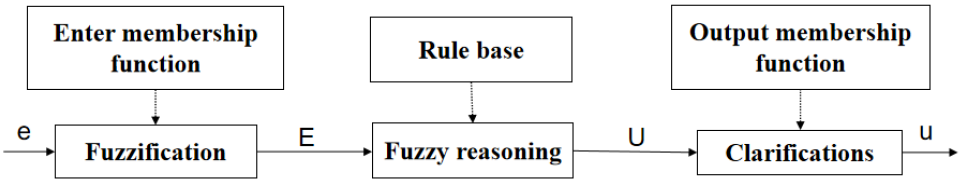

Fig. 3.2.1 Basic Schematic Diagram of fuzzy PID Control

The operations of fuzzification, fuzzy reasoning, and parameter clarifications are mainly carried out in the fuzzy controller. The two variables e, e_c are taken as inputs, which are fuzzified and divided into six parts. According to the input value of variables, the percentage of each membership degree is judged and the membership degree is determined. The domain of the specified input of $e, e_c$is [-3, 3]. The variation ranges of $\Delta k_p, \Delta k_i, \Delta k_d$ are as follows. Both Δk_p and Δk_i are [-6, 6], Δk_d is [-1, 5]. Its membership function adopts a Z-shaped membership function (zmf) on the leftmost side, a triangle membership function (trimf) in the middle, and an S-shaped membership function (smf) on the rightmost side. That is to say, the membership functions of seven input/output variables are NB (negative large), NM (negative medium), NS (negative small), Z (zero), PS (positive small), PM (positive medium), and PB (positive big), with zmf, trimf, trimf, trimf, trimf, trimf, and smf as their membership functions respectively.

Fuzzification between input and output needs to determine specific fuzzy rules. Furthermore, the formulation of fuzzy rules needs to comprehensively consider the stability, response speed, and overshoot of the system as well as their balance[7]. Generally, the proportional, integral, and differential variations are determined according to the parameters of two inputs in the formulation of fuzzy rules. Among the three inputs of the PID controller, $\Delta k_p, \Delta k_i,$ and Δk_daffect the response speed, steady deviation, and dynamic characteristics of the system respectively. In the control process, these three parameters should be adjusted according to the actual working process. For example, in the initial stage of manipulator movement, it is generally required to take a larger Δk_p value to stabilize the center of gravity as soon as possible. However, it is usually necessary to reduce the Δk_pvalue in the middle stage to prevent a large overshoot in the control process and adjust the value to a larger Δk_pvalue again at the end of control to reduce the static error; In the system, the steady deviation can be reduced by adjusting the Δk_i value. In the control process, the system often produces overshoot at the initial stage, so it is necessary to change the Δk_ivalue to weaken the integral effect. In the middle stage of manipulator movement, it is often crucial to increase the integral effect to increase the stability of the system; The differential link is a parameter introduced in consideration of the inertial of the system. The deviation of moving distance may be too large during the movement of the manipulator, while the differential coefficient can reflect the changing trend of the signal, correct its movement in time, and play the role of advanced adjustment[8].

By adjusting the proportional coefficient, integral coefficient, and differential coefficient, the optimal control of the accuracy, stability, and rapidity of the system can be realized. The three coefficients can make the system obtain good adaptability by adjusting each other.

See table 3.2.1 for specific fuzzy rules of $\Delta k_p, \Delta k_i, \Delta k_d$.

Table 3.2.1. Table of Fuzzy Rule Base

		e_c						
		NB	NM	NS	Z	PS	PM	PB
E	NB	NB/Z/PS	NB/Z/NS	NB/Z/PS	NM/Z/NB	NS/Z/NB	NS/Z/NM	Z/Z/PS
	NM	NB/NM/PS	NB/NM/NS	NM/NS/NB	NS/NS/NM	NS/NS/NM	Z/Z/NS	PS/Z/Z
	NS	NM/NB/Z	NM/NM/NS	NM/NS/NM	NB/NS/NM	Z/Z/NS	PS/PS/NS	PS/PS/Z
	Z	NM/NB/Z	NM/NM/NS	NS/NS/NS	Z/Z/NS	PS/PS/NS	PM/PM/NS	PM/PB/Z
	PS	NS/NS/Z	NS/NS/Z	Z/Z/Z	PS/PS/Z	PS/PS/Z	PM/PM/Z	PM/PB/Z
	PM	NS/Z/PB	Z/Z/NS	PS/PS/PS	PM/PS/PS	NM/PS/PS	PM/PM/PS	PB/PM/PB
	PB	Z/Z/PB	PS/Z/PM	PM/Z/PM	PM/Z/PM	PM/Z/PS	PM/Z/PS	PB/Z/PB

The fuzzy rule surface diagram of Δk_p,Δk_i, and Δk_d is shown in Figure 3.2.1.

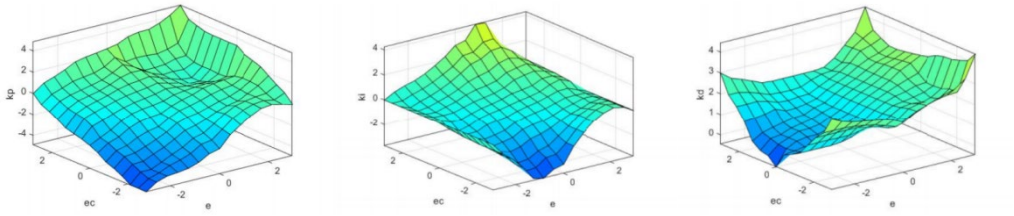

Fig. 3.2.1 Fuzzy Rule Surface Diagram

5. Matlab Simulation

5.1 Simulation Model Design

According to the transfer function of the end effector control system model of the 6R manipulator based on fuzzy PID, the movement of the end effector is simulated by Simulink. Besides, the displacement changes caused by the same external force when the end of the manipulator works are compared between conventional PID and fuzzy PID. The Simulink simulation model is shown in Figure 4.1.1. In the simulation model, the input signal is the step signal. The built-in PID by Simulink and fuzzy PID control module are used to simulate the signal.

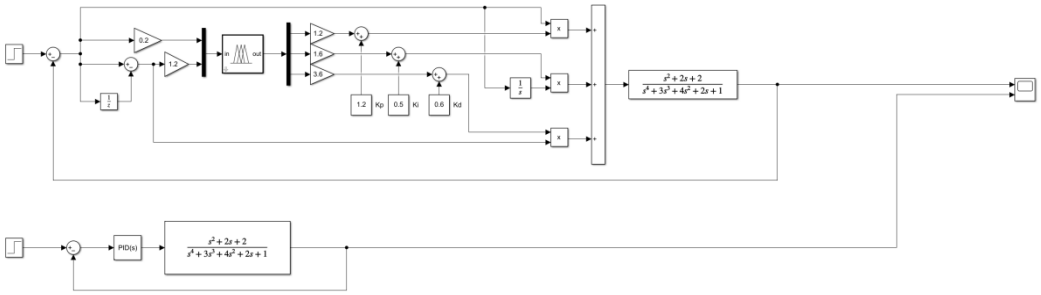

Fig. 4.1.1 Simulation Model Diagram

5.2 Performance Index Analysis

Figure 4.2.1 shows Simulink simulation results, and the specific data are shown in table 4.2.1.

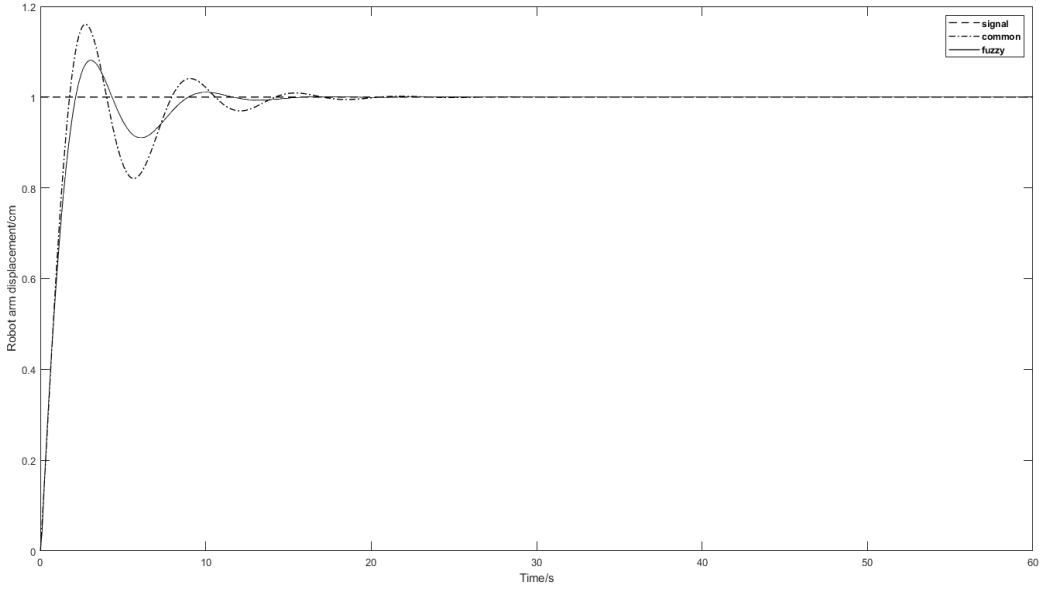

Fig. 4.2.1 Diagram of Simulink Simulation Result

Table 4.2.1 Table of Simulink Simulation Data

	First Peak	Second Peak	Attenuation Rate	Adjustment Time	Overshoot
Conventional PID	1.161 cm/2. 741 s	1.041 cm/9. 052 s	74.534%	19.896 s	16.1%
Fuzzy PID	1.081 cm/3. 000 s	1.011 cm/10. 000 s	86.419%	15.086 s	8.1%

According to the simulation results, the fuzzy PID control system has a shorter adjustment time, a smaller overshoot, a larger attenuation rate, and better three indicators compared with the conventional PID. The overshoot is only half of that of conventional PID, which shows that the displacement of fuzzy PID controlled manipulator due to external force at the end is much smaller. Thus, the manipulator controlled by fuzzy PID is more stable.

To sum up, the manipulator based on a fuzzy PID control system is better than conventional PID in accuracy, stability, and rapidity, which can control the end of the manipulator to produce smaller displacement when the same force is applied, improve the stability of the manipulator, and prevent overshoot.

5.3 Adaptability Test

Adaptability can be demonstrated from the aspects of anti-disturbance, robustness, and followingness, which are described as follows.

5.3.1 Anti-disturbance Test

The anti-disturbance of the 6R manipulator end-effector control system based on fuzzy PID is tested. The internal disturbance and external disturbance are added to better compare the control characteristics of fuzzy PID. Besides, classical PID control is added to the simulator.

For conventional and fuzzy PID control systems, internal disturbance of 0.1 is added at the 25s and internal disturbance of 0.1 is added at the 40s. The simulation results are shown in Figure 4.3.1, with the specific data shown in Table 4.3.1.

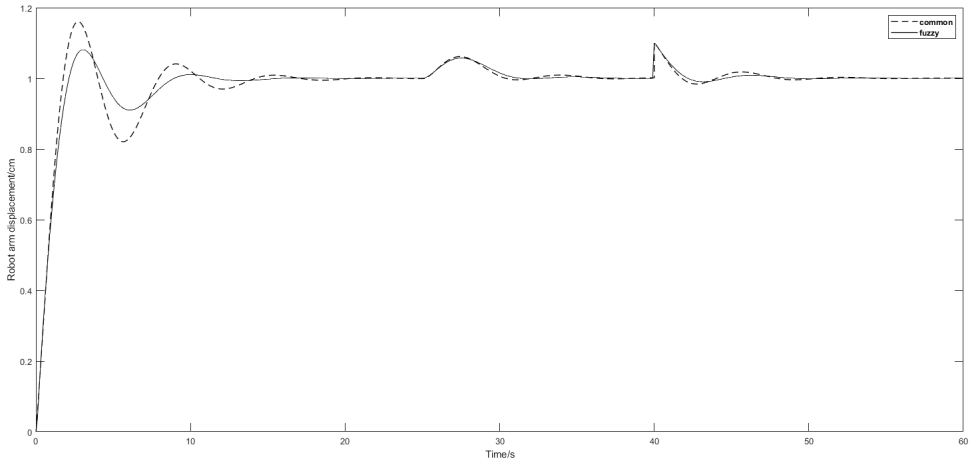

Fig. 4.3.1 Anti-disturbance Simulation Diagram

Table 4.3.1 Table of Anti-disturbance Simulation Data

	Peak Value of Internal Disturbance	Peak Value of External Disturbance	Internal Disturbance Recovery Time	External Disturbance Recovery Time
Conventional PID	1.061 cm/27. 427 s	1.101 cm/40. 003 s	19.896 s	14.784 s
Fuzzy PID	1.057 cm/27. 500s	1.099 cm/40.022 s	11.789 s	12.845 s

The simulation results show that when the system is stable, both conventional PID and fuzzy PID can recover by adding internal and external disturbances. But the recovery time of fuzzy PID is faster with the smaller fluctuation range, which proves that the manipulator controlled by fuzzy PID can

stabilize faster when the end of the manipulator is disturbed, that is, the disturbance immunity of fuzzy PID control is better.

5.3.2 Robustness Test

Robustness is the sensitivity of the influential factors that are not considered in the analysis and design stage. If a control system can meet the following requirements, including 1) low sensitivity; 2) The system that is always stable within the range of possible changes in parameters; 3) The system is robust when its performance can still meet the requirements when the parameters change[9]. Now, the controlled objects of conventional PID and fuzzy PID are changed respectively to measure the robustness of the two systems. The specific controlled objects are as follows:

$$\text{Controlled object before change:} \quad (s) = \frac{s^2+2s+2}{s^4+3s^3+4s^2+2s+1} \tag{4-1}$$

$$\text{Controlled object after change:} \quad H(s) = \frac{s^2+2s+2}{s^4+4s^3+4s^2+2s+1} \tag{4-2}$$

The simulation results are shown in Figure 4.3.2.1.

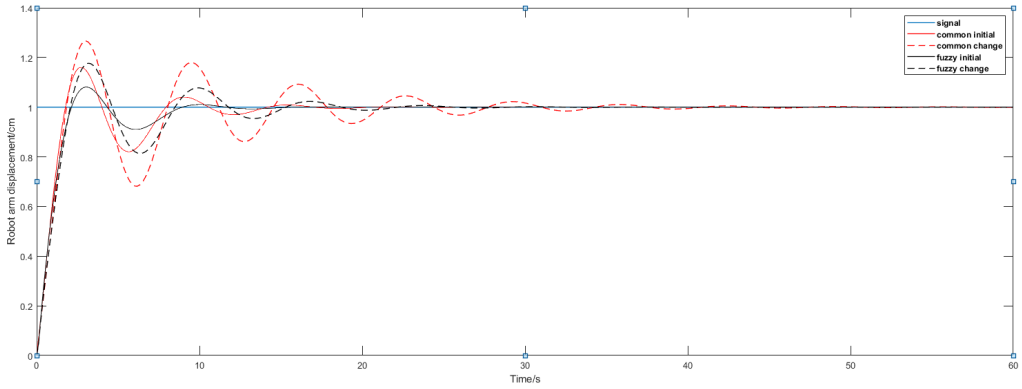

Fig. 4.3.2.1 Diagram of Robustness Test Simulation Result

The specific parameters are shown in tables 4.3.2.1 and 4.3.2.2.

Table 4.3.2.1 Simulation Data Table of Controlled Object Before Change

	First Peak	Second Peak	Attenuation Rate	Adjustment Time	Overshoot	Peak Time
Conventional PID	1.161 cm/2.741 s	1.041 cm/9.052 s	74.534%	19.896 s	16.1%	2.741 s
Fuzzy PID	1.081 cm/3.000 s	1.011 cm/10.000 s	86.419%	15.086 s	8.1%	3s

Table 4.3. 2.2 Simulation Data Table of Controlled Object After Change

	First Peak	Second Peak	Attenuation Rate	Adjustment Time	Overshoot	Peak Time
Conventional PID	1.266 cm/3.019 s	1.180 cm/9.498 s	32.330%	29.750 s	26.6%	3.019 s
Fuzzy PID	1.177 cm/3.200 s	1.078 cm/9.900s	55.932%	17.386 s	17.7%	3.200 s

By comparing the black lines, it can be concluded that the fuzzy PID control system can be well controlled for different controlled objects under the unchanged fuzzy PID control system before being stable finally, which shows that the fuzzy PID control system has robustness.

By comparing different lines, we can get that the fuzzy PID control system has a shorter adjustment time, faster response speed, smaller overshoot, and larger attenuation than the conventional PID control system in different control systems for the same controlled object, which shows that the fuzzy PID control system has stronger adaptability, that is, better robustness.

The simulation results show that the fuzzy PID control system has better robustness and is suitable for the manipulator control system with high precision and high level.

5.3.3 Followingness Test

In order to test the following performance of the control system, a step signal with an amplitude of 1 is added to the fuzzy PID control system and the conventional PID control system at the 20s. Then, a step signal with a value of -1 is added at the 40s after it is stable. The simulation results are shown in Figure 4.3.3.1 with the specific data shown in Table 4.3.3.1.

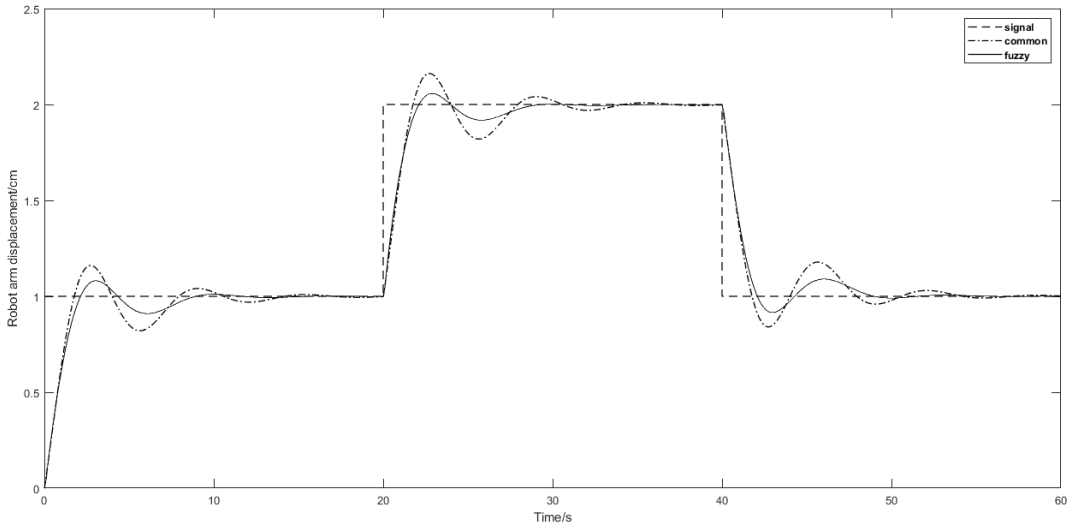

Fig. 4.3.3.1 Diagram of Followingness Test Simulation Result

Table 4.3.3.1 Table of Followingness Test Simulation Data

	First Following time	First following Time
Conventional PID	17.434 s	18.816 s
Fuzzy PID	15.955 s	15.763 s

The simulation results show that the fuzzy PID control system can follow the change of control signal faster than the conventional PID control system, that is, the manipulator controlled by fuzzy PID can adjust faster when the end of the manipulator is disturbed, which means that the fuzzy PID control system has better following performance and is suitable for the robot servo system with high precision and high requirements.

5.4 Simulation Result Analysis

According to the transfer function, the simulation results can reflect the relationship between the external force and the displacement of the end effector of the manipulator. Meanwhile, the displacement caused by the external force can reflect the stability and accuracy of the manipulator. Based on the adjustment time, overshoot, and attenuation degree, the fuzzy PID control system is superior to the conventional PID control system in rapidity, accuracy, and stability. From three aspects of anti-disturbance, robustness, and followingness, it demonstrates that fuzzy PID is better than conventional PID in adaptability. Thus, it is proved that the fuzzy PID control system can play a better role in buffer and isolation, which is suitable for the transformation of the end of the manipulator.

6. Conclusion

At present, the United States, the Soviet Union/Russia, China, Europe, and Japan have mastered the space rendezvous and docking technology, while only the United States, Russia, and China have mastered the complete rendezvous and docking technology. Europe and Japan have not mastered the

space docking technology independently due to their limited space development. After receiving technical support from the United States or Russia, they have completed some space rendezvous and docking activities[10-12]. Autonomous and automatic rendezvous and docking technology refer to the on-orbit docking task not relying on astronauts in the operation. Space rendezvous and docking are realized through their system, spacecraft, and mission control[13]. For the manipulators with the function of space rendezvous and docking, its accuracy and stability are required to be higher. According to the working situation of the 6R manipulator in reality and its shortcomings at present such as overshoot produced by the inertial assembly, this paper designs the end effector control system, introduces the Fuzzy PID control strategy, and constructs the simulation model of the control system in Simulink. By adjusting the related parameters, the simulation results achieve the expected results, which indicates that the fuzzy PID control is superior in rapidity, accuracy, and stability. Then, through the tests of anti-disturbance, robustness, and followingness, it is concluded that the new end-effector control system has good adaptability, providing a reference for the improvement of the 6R manipulator.

Up till now, the pace of exploration has never stopped ranging from space to sea. With the continuous development of human technology and the expanding exploration fields, many scenarios are no longer suitable for manual work, such as deep sea, space, and other atrocious environments. As a substitute for human activities, manipulators will inevitably explore different functions and types on the existing basis. Undoubtedly, there will also be many problems. For example, the waterproofing and communication of deep-sea manipulators, materials and synergy effects of space manipulators, etc. With the higher requirements for the performance of process control and more extensive application, classical control methods have been unable to achieve satisfactory control results, and intelligent control methods will become the development trend in the future. With the increasingly powerful functions of the manipulator, more manipulators can work in a 3D environment instead of human beings, and the control methods of the manipulator are developing to be more efficient, more stable, and more adaptive. The control method based on manipulators will mature, which can play more roles and eventually take into practice to solve more pragmatic problems.

References

[1] Flores-Abad, A., Ma, O., Pham, K. & Ulrich, S. (2014). A review of space robotics technologies for on-orbit servicing. Progress in Aerospace Sciences, 68(6),1-26.

[2] Dan, N. (1998). Canada builds space manipulators for International Space Station. Aerospace China, 3(4), 26-28.

[3] Yu D. Y., Sun, J., Ma, X. R. (2007). Suggestion on development of Chinese space manipulator technology. Spacecraft Engineering,16(4), 1-8.

[4] Laryssa, P., Lindsay, E., Layi, O. & Marius, O. (2002). International space station robotics:a comparative study of ERA,JEMRMS and MSS. 7th ESA Workshop on Advanced Space Technologies for Robotics and Automation, eASTRA.

[5] Zhang, K. F., Zhou, H., Wen, Q. P. & Sang, R. P. (2010). Review of the development of space manipulator for international space station. Chinese Journal of Space Science, 30(6), 612-619.

[6] Liu, C. H. (2005). The polishing of molds and dies using a compliance tool holder mechanism. Journal of Materials Processing Technology, 166(2), 230-236.

[7] Liu, W. G. (2021). Research and application of hydraulic servo technology based on fuzzy PID adaptive control. Hydraulics Pneumatics & Seals, 41(5), 54-56.

[8] Li, X. Y., Xiao, J. Pan, Y. P. et al. (2021). Research on leveling control system of fuzzy PID vehicle-mounted platform based on PSO. Modern Manufacturing Engineering, (2), 58-65.

[9] Richard, C. (2002). Modern Control System. 9th ed. Beijing: Science Press.

[10] Zhu, R. Z., Wang, H. F., Cong, Y. T. et al. (2013). Comparative study on Chinese and foreign rendezvous and docking technologies. Spacecraft Engineering, 22(3), 8-15.

[11] Zhao, Z. H. & Li, J. H. (2011). Automatic docking control scheme for space docking mechanism. Manned Spaceflight, 16(4), 24-27, 47.

[12] Wang, M. Xie, Y. C., Zhang, H. & Chen, C. Q. (2012). Comparison of thruster configurations for rendezvous and docking mechanism. Aerospace Control and Application, 38(3), 42-46.

[13] Liu, T., Xie, Y. C. & Hu, H. X. (2011). Application of particle filtering in relative navigation filter design for spacecraft. Aerospace Control and Application, 37(6), 19-27.